Research Article

Journal of Labelled Compounds and Radiopharmaceuticals

Received 16 July 2012, Revised 29 August 2012, Accepted 31 August 2012 Published online 11 October 2012 in Wiley Online Library

(wileyonlinelibrary.com) DOI: 10.1002/jlcr.2967

Synthesis and biological evaluation of a series of ^{99m}Tc-labeled diphosphonates as novel radiotracers with improved bone imaging

Ling Qiu, Wen Cheng, Jianguo Lin,* Liping Chen, Jun Yao, and Shineng Luo

Three radiolabeled diphosphonates, ^{99m}Tc-labeled 1-hydroxy-3-(2-propyl-1H-imidazol-1-yl)propane-1,1-diyldiphosphonic acid (PIPrDP), 1-hydroxy-4-(2-propyl-1H-imidazol-1-yl)butane-1,1-diyldiphosphonic acid (PIBDP), and 1-hydroxy-5-(2-propyl-1H-imidazol-1-yl)pentane-1,1-diyldiphosphonic acid (PIPeDP), have been designed and synthesized with good chemical yields and high radiochemical purity. Their in vitro and in vivo biological properties were investigated and compared. All radiotracers evaluated in mice showed substantial retention in bone (8.42 ± 0.53, 9.08 ± 0.65, and 10.3 ± 0.61 ID%/g, respectively) at 1 h post-injection and had rapid clearance in blood (1.9484, 1.3666, and 0.7704 ID%/g/min, respectively). ^{99m}Tc-PIBDP has the highest uptake ratio of bone-to-soft tissue at 1 h post-injection among the three radiotracers. The results indicate that ^{99m}Tc-PIBDP is the most promising bone imaging agent.

Keywords: ^{99m}Tc-labeled diphosphonates; bone imaging agent; stability; pharmacokinetics; biodistribution

Introduction

Diphosphonates (DPs) are synthetic analogs of pyrophosphate, with the backbone structure P–C–P. They are very stable and exhibit high affinity for calcified matrices, such as hydroxyapatite in bone.[1] Therefore, they have been widely used successfully as powerful inhibitors of increased bone resorption in several bone diseases, such as osteoporosis, Paget's disease, hypercalcemia of malignancy, and bone metastases of several cancers.[2–5] A number of DPs have been commercially available, such as neridronate, risedronate, zoledronate (ZL), minodronate, clodronate, pamidronate, alendronate, and ibandronate. ZL, which is considered a typical third-generation DP, is the most potent among the DPs. In preclinical models of bone resorption, ZL is at least 100 times more potent than either clodronate or pamidronate and at least 1000 times more potent than etidronate.[6] Therefore, the carbon side chains determine the pharmacological properties of the DPs.

Diphosphonates are good targeting ligands to serve as bone imaging agents.[7] For example, ^{99m}Tc-labeled methylenediphosphonate (MDP)[8] and hydroxymethylenediphosphonate (HMDP)[9] have been widely used for many years in bone scanning, which is an effective means to diagnose primary bone cancer, metastatic bone disease, osteoporosis, bone trauma, and so on.[10–13] Because of the ideal nuclear properties ($t_{1/2}$ = 6.02 h, E_γ = 140 keV) and low cost of the radionuclide technetium-99m, technetium-99m is the element of choice for more than 80% of diagnostic procedures in nuclear medicine.[14]

^{99m}Tc-labeled DPs as diagnostic agents have a number of clinical and chemical limitations,[3] such as low selectivity and relatively slow clearance from the blood and soft tissues. These properties usually lead to false negative results and extended intervals (2–6 h) between injection and bone imaging.[15] To address these problems, we need a radiopharmaceutical agent with higher affinity for bone, lower soft tissue uptake, and more rapid clearance from the blood.[16] In the last decade, we have prepared and investigated a series of ^{99m}Tc-labeled DPs with different alkyl substituents at the 2-position of the imidazole ring of ZL as new potential bone imaging agents.[17–23] These studies have showed that optimization of the alkyl substituent in the imidazole ring and the carbon chain between the imidazolyl and geminal DP groups can bring significant influence on the biological properties of ^{99m}Tc-labeled complexes.[21–23] In this work, we report on the synthesis and evaluation of a series of novel DPs with different length of the carbon chain (Scheme 1), in order to improve the bone uptake and the clearance rate from blood and soft tissues.

Experimental

Reagents, instruments, and animals

All of the chemical reagents were of analytical reagent grade. Distilled water was used for solution preparation. Fetal bovine serum (FBS) (Zhejiang Tianhang Biological Technology Co., Ltd), human serum (HS) (supplied by the affiliated Jiangyuan Hospital of Jiangsu Institute of Nuclear Medicine), and mouse serum (MS) were used for in vitro stability study. Melting points were measured on Yanaco MP-500 melting point apparatus (Shimadzu, Japan). Elemental analysis was carried out using

Key Laboratory of Nuclear Medicine, Ministry of Health, Jiangsu Key Laboratory of Molecular Nuclear Medicine, Jiangsu Institute of Nuclear Medicine, Wuxi 214063, China

**Correspondence to: Jianguo Lin, Key Laboratory of Nuclear Medicine, Ministry of Health, Jiangsu Key Laboratory of Molecular Nuclear Medicine, Jiangsu Institute of Nuclear Medicine, Wuxi 214063, China.*
E-mail: jglin@yahoo.cn

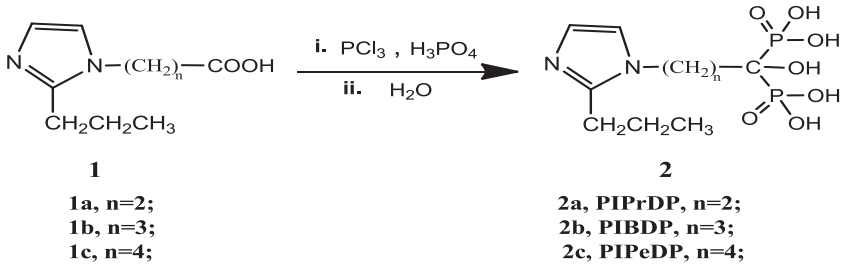

1

1a, n=2;
1b, n=3;
1c, n=4;

2

2a, PIPrDP, n=2;
2b, PIBDP, n=3;
2c, PIPeDP, n=4;

Scheme 1. Syntheses of PIPrDP, PIBDP, and PIPeDP.

an Elementar Vario EL III analyzer. Electrospray ionization mass spectrometry (ESI-MS) was determined using a Waters Platform ZMD4000 LC/MS (Waters, USA). Proton nuclear magnetic resonance (^{1}H NMR) spectra were obtained on a Bruker DRX-500 spectrometer (Bruker, Germany), and the chemical shift values were referenced to the internal tetramethylsilane. Xinhua grade 1 chromatography paper (Shanghai, China) was used for thin layer chromatography (TLC) analysis. A Packard-multi-prias γ counter (Perkins Elmer, USA) were used for counting the radioactivity. The high performance liquid chromatography (HPLC) system was equipped with a Waters 1525 binary HPLC pump (Waters, USA), a Waters 2487 dual wavelength absorbance detector (Waters, USA), and a Perkin Elmer Radiomatic 610TR radioactivity detector (Perkin Elmer, MA, USA), which were operated by Breeze and proFSA software. A reversed phase C_{18} (RP-C_{18}) column (4.6 × 250 mm; 10-μm particle size) was used for HPLC analysis (Elite Analytical Instrument Company, Dalian, China). $Na^{99m}TcO_4$ was eluted from the ^{99}Mo-^{99m}Tc generator (radiochemical purity (RCP) : 99.99%; Jiangyuan Hospital of Jiangsu Institute of Nuclear Medicine).

Normal institute of cancer research (ICR) mice (weighing 18–20 g) used for the pharmacokinetics and biodistribution studies were supplied by SLAC Laboratory Animal Company (Shanghai, China). The animal experiment was approved by the Animal Care and Ethics Committee of Jiangsu Institute of Nuclear Medicine.

Syntheses of diphosphonic acids

Three diphosphonic acids (PIPrDP, PIBDP, and PIPeDP) were synthesized according to the procedure outlined in Scheme 1 as described previously.[23–25]

Syntheses of compound 1

2-Propylimidazole (0.1 mol) was dissolved in CH_2Cl_2 (75 mL) under stirring condition. KOH (8.4 g, 0.15 mol), K_2CO_3 (13.8 g, 0.0835 mol), and $N(Bu)_4Br$ (tetrabutylammonium bromide, TBAB) (0.7 g, 0.002 mol) were added at room temperature. The homologue of ethyl bromoacetate (0.1 mol) was added, respectively. The reaction mixture was refluxed for 7 h. The solution was filtered and the filtrate was washed with brine solution. The organic phase was dried and evaporated to give the corresponding ester, which was used without further purification. HCl aqueous solution (1.2 M, 100 mL) was added to the crude ester, and the mixture was refluxed for 8 h. The solution was concentrated, and the residue was recrystallized from isopropanol to give the product **1**. *3-(2-Propyl-1H-imidazol-1-yl)propanoic acid* ***(1a)***: White solid, Yield, 46%. m.p. 149–151 °C; ESI-MS, *m/z* (%): 181 (100, $[M-H]^+$). *4-(2-Propyl-1H-imidazol-1-yl)butanoic acid* ***(1b)***: White solid, Yield, 27%. m.p. 126–129 °C; ESI-MS, *m/z* (%): 195 (100, $[M-H]^+$). *5-(2-Propyl-1H-imidazol-1-yl)pentanoic acid* ***(1c)***: Sticky substances, Yield, 24%. ESI-MS, *m/z* (%): 208 (100, $[M-H]^+$).

Syntheses of compound 2

Compound **1** (20 mmol) was dissolved in chlorobenzene (25 mL) and heated to 120 °C for 30 min, then phosphoric acid (85%, 4.2 mL) was added slowly and followed by phosphorus trichloride (7.6 mL). The reaction mixture was kept at 120 °C for 4 h. The chlorobenzene was decanted, and the yellow residue was redissolved in HCl (20 mL, 9.0 M). The mixture was refluxed for 5 h. After cooling, charcoal was added to decolor the solution. After filtration, the solvent was removed. Finally, the crude product was recrystallized from ethanol to give the white crystalline product **2**. *1-Hydroxy-3-(2-propyl-1H-imidazol-1-yl)propane-1,1-diyldiphosphonic acid* ***(2a)***: Yield, 40%. mp 242–245 °C; ESI-MS, *m/z* (%): 327(100, $[M-H]^+$). ^{1}H NMR (400 MHz, D_2O): δ7.39 (d, *J* = 2.0 Hz, 1H, CH-ring), 7.26 (d, *J* = 2.0 Hz, 1H, CH-ring), 4.39–4.43 (m, 2H, N–CH_2), 2.92–2.96 (t, *J* = 7.6 Hz, 2H, ring-CH_2), 2.34–2.45 (m, 2H, OH–C–CH_2), 1.71–1.80 (m, 2H, $CH_2CH_2CH_3$), 0.91–0.95 (t, *J* = 7.6 Hz, 3H, –CH_3). *1-Hydroxy-4-(2-propyl-1 H-imidazol- 1-yl)butane-1, 1-diyldiphosphonic acid* ***(2b)***: Yield, 35%. mp 212–214 °C; ESI-MS, *m/z* (%): 341(100, $[M-H]^+$). ^{1}H NMR (400 MHz, D_2O): δ7.32 (d, *J* = 2.0 Hz, 1H, CH-ring), 7.24 (d, *J* = 2.0 Hz, 1H, CH-ring), 4.06–4.10 (t, *J* = 7.2 Hz, 2H, N–CH_2), 2.87–2.90 (t, *J* = 7.2 Hz, 2H, ring-CH_2), 1.91–1.98 (m, 2H, OH–C–CH_2), 1.76–1.83 (m, 2H, $CH_2CH_2CH_3$), 1.66–1.73 (m, 2H, N–$CH_2CH_2CH_2$), 1.58–1.62 (m, *J* = 6.8 Hz, 2H, –CH_2), 0.88–0.91 (t, *J* = 7.2 Hz, 3H, –CH_3). *1-Hydroxy-5-(2-propyl-1H-imidazol-1-yl)pentane-1,1-diyldiphosphonic acid* ***(2c)***: Yield, 25%. m.p. 217–221 °C; ESI-MS, *m/z* (%): 355 (100, $[M-H]^+$). ^{1}H NMR (400 MHz, D_2O): δ7.34 (d, *J* = 2.0 Hz, 1H, CH-ring), 7.27 (d, *J* = 2 Hz,1H, CH-ring), 4.08–4.12 (t, 2H, *J* = 7.2 Hz, N–CH_2), 3.56–3.62 (m, 2H, OH–C–CH_2), 2.89–2.93 (dd, *J* = 7.2 Hz, 2H, ring-CH_2), 1.81–1.93 (m, 2H, N–CH_2–CH_2), 1.60–1.76 (m, 2H, –$CH_2CH_2CH_3$), 1.10–1.14 (m, 2H, –CH_2), 0.90–0.94 (t, *J* = 7.2 Hz, 3H, –CH_3).

Radiolabeling

Compounds 2a-2c (5 mg, dissolved in 0.1 mL 0.2 M NaOH solution), $SnCl_2{\cdot}2H_2O$ solution (100 μL, freshly prepared, 10 mg $SnCl_2{\cdot}2H_2O$ dissolved in 10.0 mL 0.5 M HCl solution), and $Na^{99m}TcO_4$ (74.0 MBq freshly eluted) were added into a penicillin vial in turn. The pH of the mixture was adjusted to pH = 6.0 by adding 0.2 M phosphate buffer solution (PBS). The final volume of the solution was adjusted to 2 mL by water. The reaction mixture was heated at 70 °C for 30 min.

Quality control

The radiolabeling yield (RLY) and RCP of ^{99m}Tc-DPs were determined by TLC and HPLC analyses, respectively.

Thin layer chromatography analysis

Radiolabeling yields of ^{99m}Tc-PIPrDP, ^{99m}Tc-PIBDP, and ^{99m}Tc-PIPeDP were determined using TLC analysis. Strips of Xinhua No.1 paper chromatography of 13 cm long and 0.5 cm wide were marked at a distance of 1.5 cm from the lower end and lined into sections 1 cm each up to 10 cm. About 3 μL of ^{99m}Tc-PIPrDP, ^{99m}Tc-PIBDP, or ^{99m}Tc-PIPeDP solution was applied with a syringe at 1.5 cm from the bottom of the paper strip, and then the strip was developed in distilled water and acetone. After complete development, the strip was dried and assayed by Mini-Scan radio-TLC.

High performance liquid chromatography analysis

Radiochemical purities of ^{99m}Tc-PIPrDP, ^{99m}Tc-PIBDP, and ^{99m}Tc-PIPeDP were determined by HPLC analysis. Each sample was filtered through a millipore filter (0.22 μm) carefully and 10 μL of sample was injected into the HPLC column. The elution conditions are as follows: isocratic of

70% TBAB (5 mmol/L) aqueous solution and 30% CH_3CN, the flow rate of 1 mL/min, and a Cd (Te) detector for radioanalysis.

In vitro stability

In vitro stability of ^{99m}Tc-DPs was studied in PBS (pH = 7.4), FBS, HS, or MS for 1–6 h. Briefly, 200 μL (3.7 MBq) of ^{99m}Tc-PIPrDP, ^{99m}Tc-PIBDP, and ^{99m}Tc-PIPeDP were added into 200 μL of PBS, FBS, HS, or MS, respectively. After incubation at 37 °C for 1–6 h, an aliquot of the PBS solution was taken directly, and the radioactivity was analyzed by TLC. For the solution of FBS, HS, or MS, an aliquot was added into 100 μL of 50% trifluoroacetic acid in water. After centrifugation, the upper solution was taken for TLC analysis.

Octanol–water partition coefficient

Octanol–water partition coefficient (log P_{OW}) was determined for ^{99m}Tc-PIPrDP, ^{99m}Tc-PIBDP, and ^{99m}Tc-PIPeDP at pH = 7.4 by measuring the radioactivity of the radiolabeled compound in octanol and PBS, respectively, at equilibrium. ^{99m}Tc-PIPrDP, ^{99m}Tc-PIBDP, or ^{99m}Tc-PIPeDP solution was diluted with PBS (100 μL + 900 μL), respectively. The solution was mixed with 1 mL octanol, vortexed for 5 min, and centrifuged at 4000 rpm for 5 min to ensure complete separation of layers. An aliquot of organic and aqueous phases (100 μL each) were collected, and the radioactivity was measured with a γ counter. The log P_{OW} was calculated using the formula log P_{OW} = log (octanol CPM / PBS CPM).[26] The reported value is the average obtained from three independent experiments.

Plasma protein binding assay

^{99m}Tc-PIPrDP, ^{99m}Tc-PIBDP or ^{99m}Tc-PIPeDP (100 μL, 37 KBq) was mixed with a human plasma solution (100 μL) in the centrifuge tube. After the mixture was incubated at 37 °C for 2 h, the plasma protein was precipitated by adding 1 mL trifluoroacetic acid solution in water (250 g/L). The supernatant and precipitate were separated by centrifugation at 3000 rpm for 5 min. The radioactivities of both phases were measured by a γ counter separately. The aforementioned procedure was repeated three times. The percentage of protein binding was determined by the following equation: Plasma binding % = (Precipitate CPM / [Precipitate CPM + Supernatant CPM]) *100%.

Pharmacokinetic studies

For pharmacokinetics studies, ^{99m}Tc-PIPrDP, ^{99m}Tc-PIBDP, or ^{99m}Tc-PIPeDP (7.4 MBq, 0.2 mL) was administered to the mice via intravenous injection through the tail vein. A series of blood samples (20 μL) were collected in microcap tubes by nicking the tail with a needle at 2, 5, 10, 15, 30, 60, 120, 180, 240, and 360 min after injection. The radioactivity of each blood sample was counted and expressed as a percentage of the injected dose per gram of blood (%ID/g). The radioactivity was expressed as a function of time, and pharmacokinetics parameters were calculated using the 3P97 program (Chinese Mathematical Pharmacology, 1997, Beijing, China). Biexponential equation was used to fit the curve: $C = Ae^{-\alpha t} + Be^{-\beta t}$, where C is the plasma level of the tracer at any given time t; A and B are constants; α and β are rate constants of distribution and elimination phases.

In vivo distribution

^{99m}Tc-DPs (7.4 MBq, 0.2 mL) were administered to 30 institute of cancer research mice (five mice for each group) via the tail vein injection. The mice were sacrificed by decapitation at 5, 15, 30, 60, 120, and 240 min post-injection. Interested organs (containing joints and femur) were collected and weighed, and 200 μL of blood was taken from the carotid artery. The radioactivity of each sample was measured by a γ counter. The distribution of each radiotracer in different organs was calculated and expressed as the percentage uptake of the injected dose per gram of organ (%ID/g) and the uptake rations of bone to other tissues were obtained from the ID%/g values.

Statistical analysis

Statistical analysis of the bone uptake and uptake ratios of bone to heart, liver, spleen, blood, and muscle was performed using the Student's *t*-test for unpaired data (GraphPad Prism 5.0). A 95% confidence level was chosen to determine the significance between groups, with $p < 0.05$ being significantly different.

Results and discussion

Chemistry and radiolabeling

PIPrDP, PIBDP, and PIPeDP were synthesized by four steps according to the previous method (Scheme 1).[23] In the first step, compound **1** was prepared through the *N*-alkylation reaction. To accelerate the reaction rate and achieve a satisfactory yield, TBAB was added to the reaction system as a phase transfer catalyst.[27] Compound **2** was obtained through the phosphine acidification reaction of the carboxylic acid. The speed of adding PCl_3 had critical effect on the yield of the reaction. If the addition is fast, the reaction may be hard to control, and the yield was also low. Otherwise, the reaction time may be too long. A moderate speed (about 0.4 mL/min) was selected to control the reaction temperature and increase the yield.

PIPrDP, PIBDP, and PIPeDP were further labeled with $^{99m}TcO_4^-$ with the reducing agent stannous chloride. The pH value was very important for the radiolabeling. When the acidity is high (pH = 1–3), the RLY and RCP are less than 90%, because of incomplete reduction of $^{99m}TcO_4^-$ under strong acidic conditions. When the pH is larger than 6, over-reduction of $^{99m}TcO_4^-$ into a colloid of ^{99m}Tc predominates, the RLY and RCP decrease significantly. The best pH range is 4–6, the RLY and RCP are more than 95%. This labeling method meets the clinical requirement used for the production of other standard ^{99m}Tc-labeled DPs, such as ^{99m}Tc-MDP.

Quality control

We used TLC to monitor the progress of the radiolabeling reactions and check the purity of the radiolabeled compounds. All of the chemical species involved in the radiolabeling reactions were separated by TLC method. From TLC analysis, the three radiotracers showed similar results. With the distilled water as eluate, $^{99m}TcO_2{\cdot}nH_2O$ remained at the origin (R_f = 0–0.1), whereas $Na^{99m}TcO_4$ and ^{99m}Tc-DPs both migrated with the solvent front (R_f = 0.7–0.9). When acetone was used, $^{99m}TcO_2{\cdot}nH_2O$ and ^{99m}Tc-DPs remained at the origin (R_f = 0–0.1), $Na^{99m}TcO_4$ migrated with the solvent front (R_f = 0.9–1.0). At optimal radiolabeling conditions, TLC showed that $Na^{99m}TcO_4$ was completely reduced and ^{99m}Tc-colloidal amount was less than 2% (Figure 1(a)).

We also used HPLC to monitor the progress of the radiolabeling reactions and to check the purity of the radiolabeled compounds. Because these ^{99m}Tc-DPs are all ionic and highly polar, they showed no retention on standard reversed phase HPLC column, such as RP-18.[28] A little amount of TBAB was added in the mobile phase to serve as the ion pair reagent to improve the retention time of ^{99m}Tc-DPs and free technetium. HPLC analysis revealed that the retention time of free technetium ($Na^{99m}TcO_4$) was 9.8 min, whereas that of ^{99m}Tc-DPs was 3.4 ± 0.2 min. (Figure 1(b)). For each radiotracer synthesized, only one single peak was observed. This clearly showed that the complexes were pure, no residual $Na^{99m}TcO_4$ or other impurities.[25] Both TLC and HPLC showed that RCPs of three ^{99m}Tc-DPs were all larger than 98%.

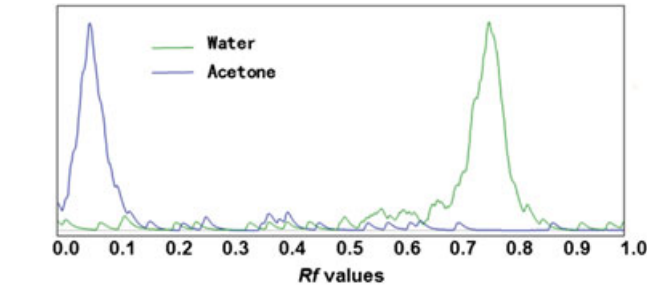

(a)

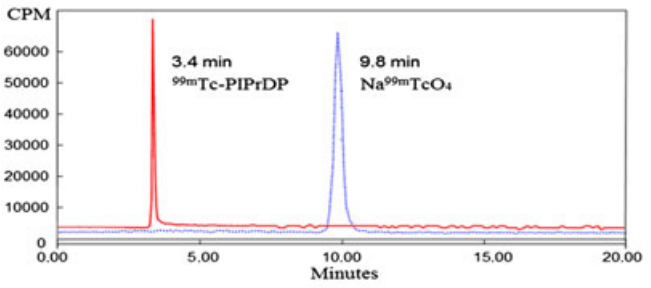

(b)

Figure 1. (a) Thin layer chromatography of ^{99m}Tc-PIPrDP in water and acetone; (b) HPLC of ^{99m}Tc-PIPrDP and $Na^{99m}TcO_4$.

Hence, these radiolabeled compounds were used immediately without further purification for both in vitro and in vivo studies.

In vitro stability

The stability was evaluated by measuring the RCP of each radiotracer using TLC analysis. More than 95% of ^{99m}Tc-PIPrDP, ^{99m}Tc-PIBDP, and ^{99m}Tc-PIPeDP remained intact in the PBS, FBS, HS, and MS after 6 h of incubation (Figure 2). Therefore, ^{99m}Tc-DPs are stable enough for human or rodent studies for up to 6 h.

log P_{OW} and plasma protein binding

Octanol–water partition coefficients (log P_{OW}) of ^{99m}Tc-PIPrDP, ^{99m}Tc-PIBDP, and ^{99m}Tc-PIPeDP were determined to be −1.58, −1.56, and −1.53, respectively. The rather similar log P_{OW} values reflect the structural analogy of three ^{99m}Tc-DPs. Usually, higher lipid molecules have positive effects on the bone resorption in the bone-binding model.[29] In our previous studies, we found that complexes with longer alkyl substituent in the imidazole ring had higher lipophilicity.[23,30] Because log P_{OW} is an important parameter for assessing the biological distribution of these complexes,[31] we speculate that the new ^{99m}Tc-DPs have larger positive effects on the bone uptake than the previously synthesized DPs.

Almost no difference was observed among the plasma protein binding of these complexes although the carbon chain increased from 2 to 4. The percent of plasma protein binding was 25.2 ± 0.7, 26.2 ± 0.5, 25.8 ± 0.9 for ^{99m}Tc-PIPrDP, ^{99m}Tc-PIBDP, and ^{99m}Tc-PIPeDP, respectively. This may be because of the structural analogy of these ^{99m}Tc-DPs, as observed from log P_{OW} study described earlier. In general, the plasma protein binding efficiency has significant influence on the bone uptake of the radiotracer[32] and analysis of ^{99m}Tc-DPs in the whole blood is the key to the development of novel drugs for clinical use.[33]

Pharmacokinetic studies

The time-activity curve of radioactivity in blood of mice for each ^{99m}Tc-DP during 6 h post-injection follows a double exponential curve (Figure 3), with $C = 5.39e^{-0.055t} + 0.85e^{-0.010t}$, $C = 8.49e^{-0.053t} + 0.85e^{-0.075t}$, and $C = 17.27e^{-0.056t} + 0.737e^{-0.0042t}$. The $T_{1/2\alpha}$ value is correlated with the molecular size, where the smaller the compound, the shorter is the distribution half-life (Table 1).[34] We believe that when the molecular weight is smaller, the permeability into the organs and tissues from the blood is faster. Consequently, the distribution half-life ($T_{1/2\alpha}$) is shorter. On the other hand, the elimination half-life $T_{1/2\beta}$ basically followed the same trend. The elimination is primarily through the renal filtration, and larger molecules would be removed slower than the smaller ones.

Biodistribution studies

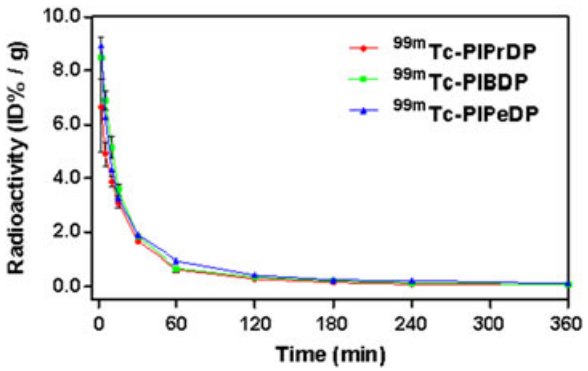

Figure 3. The time activity curve of ^{99m}Tc-DPs in the blood of mice ($n = 5$, mean ± SD).

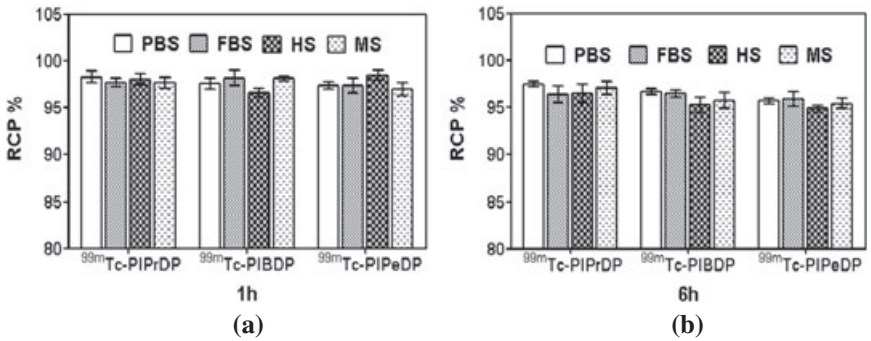

(a) (b)

Figure 2. In vitro stability of ^{99m}Tc-DPs in phosphate buffer solution (PBS), fetal bovine serum (FBS), human serum (HS) and mouse serum (MS) after 1 and 6 h, respectively.

Table 1. Pharmacokinetics parameters of ^{99m}Tc-DPs

^{99m}Tc-DPs	$T_{1/2\alpha}$ (min)	$T_{1/2\beta}$ (min)	K_e (min^{-1})	AUC (ID%/g*min)	CL (ID%/g/min)
^{99m}Tc-PIPrDP	13.467	75.294	0.0329	189.89	1.9484
^{99m}Tc-PIBDP	15.957	91.276	0.0344	270.77	1.3666
^{99m}Tc-PIPeDP	21.232	164.82	0.0375	480.24	0.7704

$T_{1/2\alpha}$, distribution half-life; $T_{1/2\beta}$, elimination half-life; K_e, elimination rate constant; AUC, area under the time activity curve; CL, total clearance rate.

The ^{99m}Tc-DPs mainly accumulated in the skeleton, particularly in the joint (Table 2). All ^{99m}Tc-DPs reached the skeleton within 5 min post-injection. At 60 min post-injection, in general, the uptake of ^{99m}Tc-DPs in the joint reached the peak at 10.3 ± 1.25 (at 120 min, 13.0 ± 0.74), 12.3 ± 1.53, and 13.4 ± 1.43 ID%/g for ^{99m}Tc-PIPrDP, ^{99m}Tc-PIBDP, and ^{99m}Tc-PIPeDP, respectively. Throughout the study period, no sign of toxicity was observed for these ^{99m}Tc-DPs. This is consistent with the general observation that ZL has low toxicity and can be used therapeutically at a high dose.[35,36] Therefore, the most suitable time of the new agents for bone imaging is 60 min post-injection. This represents significant shortening of the time interval between injection and bone scanning.

The extension of the carbon chain in this series of ^{99m}Tc-DPs increased their bone uptake. That is, the bone uptake of ^{99m}Tc-PIPeDP is larger than ^{99m}Tc-PIPrDP and ^{99m}Tc-PIBDP. Compared with the clinically widely used bone imaging agent ^{99m}Tc-MDP, the bone uptake of these ^{99m}Tc-DPs at 30, 60, and 120 min post-injection were all higher than those of ^{99m}Tc-MDP, which were 3.26, 4.79, and 3.87%ID/g, respectively.[37] This is consistent with what we have observed before in analogous systems.[31]

The uptakes of ^{99m}Tc-PIBDP in most soft tissues were always smaller than ^{99m}Tc-PIPrDP and ^{99m}Tc-PIPeDP, such as in the heart, liver, spleen, kidney, and muscle. However, all these ^{99m}Tc-DPs have higher uptake in the kidney. At 2 h post-injection, the kidney uptakes of the three radiotracers were still 5.71 ± 0.17, 3.29 ± 0.10, and 5.52 ± 0.28 ID%/g, respectively. One possibility is that the filtration rate of glomerulus is slow, and the reabsorption is not

Table 2. Biodistribution of ^{99m}Tc-DPs in mice as a function of time (Mean ± SD, n = 5, ID%/g)

	Time post-injection					
Tissue	5 min	15 min	30 min	60 min	120 min	240 min
^{99m}Tc-PIPrDP						
Heart	3.11 ± 0.19	1.31 ± 0.08	0.73 ± 0.02	0.44 ± 0.01	0.30 ± 0.02	0.30 ± 0.01
Liver	3.10 ± 0.24	2.17 ± 0.08	2.18 ± 0.21	2.17 ± 0.04	1.88 ± 0.10	2.23 ± 0.11
Spleen	1.55 ± 0.10	0.73 ± 0.01	0.60 ± 0.05	0.44 ± 0.03	0.46 ± 0.03	0.32 ± 0.02
Kidney	11.5 ± 0.17	8.30 ± 0.34	6.40 ± 0.25	5.88 ± 0.06	5.71 ± 0.17	4.78 ± 0.22
Femur	4.06 ± 0.19	3.58 ± 0.16	3.93 ± 0.41	4.16 ± 0.19	4.38 ± 0.15	4.41 ± 0.19
Joint	7.96 ± 0.38	7.91 ± 1.54	9.56 ± 2.05	10.3 ± 1.25	13.0 ± 0.74	11.4 ± 0.85
Muscle	1.97 ± 0.02	0.81 ± 0.01	0.55 ± 0.01	0.25 ± 0.02	0.12 ± 0.02	0.17 ± 0.00
Blood	8.73 ± 0.24	4.64 ± 0.07	2.71 ± 0.12	1.00 ± 0.02	0.37 ± 0.04	0.13 ± 0.01
All bone	6.85 ± 0.07	6.68 ± 0.25	7.61 ± 1.12	8.42 ± 0.53	10.2 ± 0.03	8.60 ± 1.00
^{99m}Tc-PIBDP						
Heart	2.06 ± 0.19	0.86 ± 0.05	0.40 ± 0.10	0.30 ± 0.02	0.14 ± 0.00	0.10 ± 0.01
Liver	1.10 ± 0.08	0.95 ± 0.11	0.68 ± 0.14	0.77 ± 0.02	0.40 ± 0.01	0.41 ± 0.05
Spleen	1.00 ± 0.08	0.68 ± 0.05	0.33 ± 0.01	0.26 ± 0.04	0.15 ± 0.00	0.13 ± 0.00
Kidney	3.90 ± 0.34	3.71 ± 0.26	4.11 ± 0.44	3.70 ± 0.13	3.29 ± 0.10	3.36 ± 0.07
Femur	3.66 ± 0.21	3.31 ± 0.25	4.08 ± 0.11	4.38 ± 0.41	4.00 ± 0.18	3.60 ± 0.01
Joint	6.20 ± 0.36	7.51 ± 1.08	7.46 ± 0.57	12.3 ± 1.53	7.88 ± 0.35	9.49 ± 0.85
Muscle	1.01 ± 0.06	0.50 ± 0.06	0.38 ± 0.00	0.22 ± 0.03	0.12 ± 0.02	0.06 ± 0.00
Blood	6.42 ± 0.36	2.72 ± 0.12	1.01 ± 0.00	0.84 ± 0.03	0.18 ± 0.00	0.07 ± 0.01
All bone	4.79 ± 0.35	6.14 ± 0.87	5.62 ± 0.49	9.08 ± 0.65	6.64 ± 0.84	6.80 ± 0.39
^{99m}Tc-PIPeDP						
Heart	1.91 ± 0.10	1.25 ± 0.04	0.57 ± 0.04	0.44 ± 0.01	0.26 ± 0.02	0.34 ± 0.03
Liver	2.24 ± 0.19	2.04 ± 0.03	1.62 ± 0.04	1.49 ± 0.11	1.13 ± 0.06	1.76 ± 0.16
Spleen	1.46 ± 0.04	0.82 ± 0.05	0.47 ± 0.01	0.39 ± 0.01	0.32 ± 0.05	0.26 ± 0.06
Kidney	10.5 ± 0.30	7.39 ± 0.63	6.19 ± 0.19	5.46 ± 0.34	5.52 ± 0.28	5.94 ± 0.13
Femur	4.63 ± 0.26	4.57 ± 0.03	4.56 ± 0.19	5.31 ± 0.17	4.55 ± 0.06	6.51 ± 0.60
Joint	7.25 ± 0.81	7.55 ± 0.96	10.9 ± 1.21	13.4 ± 1.43	11.6 ± 0.77	12.5 ± 2.26
Muscle	1.44 ± 0.10	0.69 ± 0.09	0.34 ± 0.01	0.25 ± 0.05	0.15 ± 0.01	0.10 ± 0.01
Blood	6.51 ± 0.07	3.38 ± 0.03	1.49 ± 0.04	0.51 ± 0.04	0.17 ± 0.03	0.13 ± 0.04
All bone	6.75 ± 0.07	7.54 ± 1.31	7.92 ± 0.99	10.3 ± 0.61	10.0 ± 0.33	10.5 ± 1.32

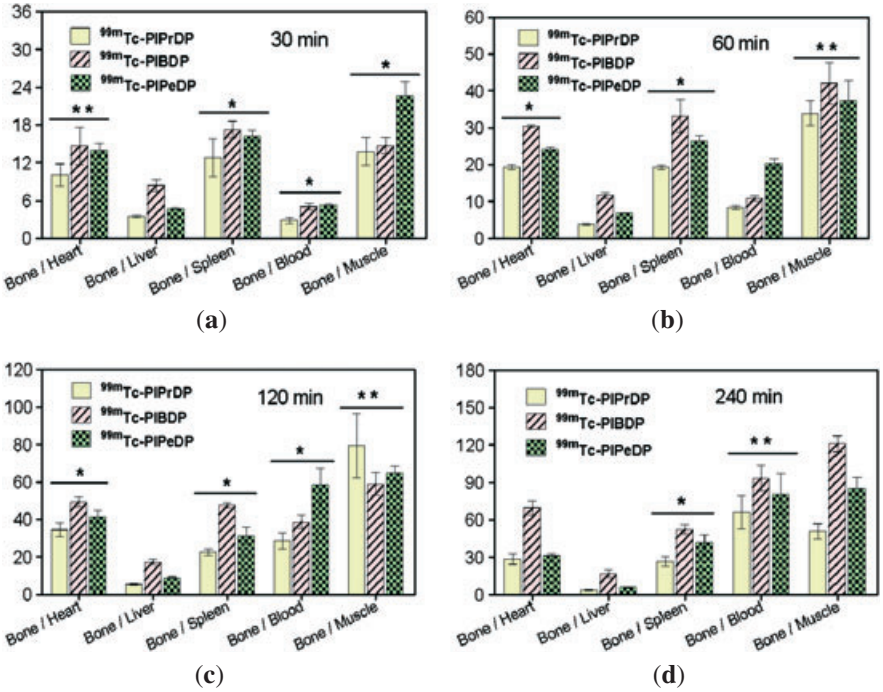

Figure 4. Uptake ratios of bone to soft tissues at different time post-injection of ^{99m}Tc-DPs. Data were expressed as mean ± SD. Statistical differences among three groups were evaluated using unpaired Student's *t*-test (*, $p < 0.05$; **, $p < 0.01$).

Table 3. Statistical difference among the bone uptake of three ^{99m}Tc-DPs assessed by the unpaired Student's *t*-test

Time	5 min	15 min	30 min	60 min	120 min	240 min
t	9.141	16.65	9.784	16.83	7.748	8.082
p	0.0118	0.0036	0.0103	0.0035	0.0163	0.015

significant.[38] Moreover, the accumulation of ^{99m}Tc-DPs in the liver was also higher in the period of investigation, suggesting that these radiotracers were not only cleared through the kidney but also eliminated from the liver. This kind of metabolic pathway may increase the burden on the liver. The uptake of ^{99m}Tc-PIPrDP, ^{99m}Tc-PIBDP, and ^{99m}Tc-PIPeDP in blood cleared rapidly (Table 2). This is also consistent with the previous pharmacokinetic investigation of other ^{99m}Tc-DPs.[23]

The uptake ratios of bone to heart, liver, spleen, and muscle for the complex ^{99m}Tc-PIBDP were higher than those of ^{99m}Tc-PIPrDP and ^{99m}Tc-PIPeDP at any given time post-injection (Figure 4). ^{99m}Tc-PIBDP has both higher selective uptake in the skeletal system and lower background uptake in soft tissues. Therefore, it has great potential to shorten the interval between injection and imaging, lessening the burden on patients in terms of examination time when compared with the clinically widely used ^{99m}Tc-MDP agent. Statistical analysis of bone uptakes and uptake ratios of bone to soft tissues (heart, liver, spleen, blood, muscle) of three radiopharmaceuticals (Table 3 and Figure 4) revealed that they were significantly different.

Conclusions

Three novel technetium-99m labeled zoledronic acid derivatives (^{99m}Tc-PIPrDP, ^{99m}Tc-PIBDP, and ^{99m}Tc-PIPeDP) were synthesized with high RLY and purity. They had excellent stability in vitro and rapid blood clearance in vivo. Among the three compounds examined, the carbon chain between the imidazolyl and geminal DP groups determined the radioactivity uptake of bone and soft tissue. At 1 h post-injection, ^{99m}Tc-PIBDP showed a higher selective bone uptake and lower soft tissue uptake, therefore uptake ratios of bone to soft tissues. It has the great potential to serve as bone scanning agent among three designed ^{99m}Tc-DPs. We will continue to explore ^{99m}Tc-PIBDP as a novel SPECT imaging agent in larger animals and animals with bone metastases.

Acknowledgements

We are very grateful to the National Natural Science Foundation of China (20801024 and 21001015), Natural Science Foundation of Jiangsu Province (BK2009077), and Key Medical Talent Project of Jiangsu Province (RC2011097) for their financial support.

Conflict of Interest

The authors did not report any conflict of interest.

References

[1] A. Jung, S. Bisaz, H. Fleisch, *Calc. Tiss. Res.* **1973**, *11*, 269.
[2] G. A. Rodan, T. J. Martin, *Science* **2000**, *289*, 1508.
[3] S. Vasireddy, A. Talwarkar, H. Miller, *Clin. Rheumatol.* **2003**, *22*, 376.
[4] R. E. Coleman, E. V. McCloskey, *Bone* **2011**, *49*, 71.
[5] A. Lipton, *Expert Opin. Pharmacother.* **2011**, *12*, 749.
[6] M. R. Smith, *Urol. Oncol.: Semin. Orig. Investig.* **2008**, *26*, 420.
[7] S. S. Jurisson, J. D. Lydon, *Chem. Rev.* **1999**, *99*, 2205.

[8] G. Subramanian, J. G. McAfee, R. J. Blair, F. A. Kallfelz, F. D. Thomas, *J. Nucl. Med.* **1975**, *16*, 744.
[9] J. A. Bevan, A. J. Tofe, J. J. Benedict, M. D. Francis, B. L. Barnett, *J. Nucl. Med.* **1980**, *21*, 961.
[10] F. M. Paes, A. N. Serafini, *Semin. Nucl. Med.* **2010**, *40*, 89.
[11] V. J. Lewington, *J. Nucl. Med.* **2005**, *46*, 38S.
[12] N. Pandit-Taskar, M. Batraki, C. R. Divgi, *J. Nucl. Med.* **2004**, *45*, 1358.
[13] W. A. Volkert, T. J. Homan, *Chem. Rev.* **1999**, *99*, 2269.
[14] P. Elisa, D. G. Joao, P. C. C. Maria, S. Isabel, *Mol. Biosyst.* **2011**, *7*, 2950.
[15] C. Love, A. S. Din, M. B. Tomas, T. P. Kalapparambath, C. J. Palestro, *Radiographics* **2003**, *23*, 341.
[16] K. Ogawa, T. Mukai, Y. Inoue, M. Ono, H. D. Saji, *J. Nucl. Med.* **2006**, *47*, 2042.
[17] S. N. Luo, H. Y. Wang, M. H. Xie, *Chin. J. Nucl. Med.* **2005**, *6*, 342.
[18] G. S. Niu, S. N. Luo, X. H. Yan, M. Yang, W. Z. Ye, H. Y. Wang, *Nucl. Tech.* **2008**, *31*, 698. (in Chinese)
[19] C. Q. Chen, S. N. Luo, J. G. Lin, M. Yang, W. Z. Ye, L. Qiu, *Nucl. Sci. Tech.* **2009**, *20*, 302.
[20] J. G. Lin, S. N. Luo, C. Q. Chen, L. Qiu, Y. Wang, W. Cheng, *Appl. Radiat. Isot.* **2010**, *9*, 1616.
[21] Y. Wang, S. N. Luo, J. G. Lin, L. Qiu, W. Cheng, H. Z. Zhai, B. B. Nan, W. Z. Ye, Y. Y. Xia, *Appl. Radiat. Isot.* **2011**, *69*, 1169.
[22] J. G. Lin, L. Qiu, W. Cheng, S. N. Luo, W. Z. Ye, *Nucl. Med. Biol.* **2011**, *38*, 619.
[23] L. Qiu, W. Cheng, J. G. Lin, S. N. Luo, L. Xue, J. Pan, *Molecules* **2011**, *16*, 6165.
[24] L. Widler, K. A. Jaeggi, M. Glatt, K. Müller, R. Bachmann, M. Bisping, A. R. Born, R. Cortesi, G. Guiglia, H. Jeker, *J. Med. Chem.* **2002**, *45*, 3721.
[25] K. Verbeke, J. Rozenski, B. Cleynhens, H. Vanbilloen, T. Groot, N. Weyns, G. Bormans, A. Verbruggen, *Bioconjug. Chem.* **2002**, *13*, 16.
[26] M. I. M. Prata, A. C. Santos, S. W. A. Bligh, A. H. M. S. Chowdhury, C. F. G. C. Geraldes, J. J. P. Lima, *Nucl. Med. Biol.* **2000**, *27*, 605.
[27] X. P. Hui, L. M. Zhang, Z. Y. Zhang, *Chin. J. Org. Chem.* **1999**, *99*, 67.
[28] V. Katrin, V. Torsten, A. Helmut, H. Jendrik, S. Arne, K. Uwe, *J. Chromatogr. B* **2011**, *879*, 2073.
[29] Y. H. Zhang, R. Cao, F. L. Yin, M. P. Hudock, R. T. Guo, K. Krysiak, S. Mukherjee, Y. G. Gao, H. Robinson, Y. C. Song, J. H. No, K. Bergan, A. Leon, L. Cass, A. Goddard, T. K. Chang, F. Y. Lin, E. V. Beek, S. Papapoulos, A. H. J. Wang, T. Kubo, M. Ochi, D. Mukkamala, E. Oldfield, *J. Am. Chem. Soc.* **2009**, *131*, 5153.
[30] J. G. Lin, L. Qiu, W. Cheng, S. N. Luo, L. Xue, S. Zhang, *Appl. Radiat. Isotopes.* **2012**, *70*, 848.
[31] K. Valko, *J. Chromatogr. A* **2004**, *1037*, 299.
[32] J. Kroesbergen, A. M. P. Roozen, M. R. Wortelboer, W. J. Gelsema, C. L. DeLigny, *Nucl. Med. Biol.* **1988**, *5*, 479.
[33] J. A. Wong, K. W. Renton, J. F. Crocker, P. A. O'Regan, P. D. Acott, *Biomed. Chromatogr.* **2004**, *18*, 98.
[34] D. Wang, M. Sima, R. L. Mosley, J. P. Davda, N. Tietze, S. C. Miller, P. R. Gwilt, P. Kopeckova, *Mol. Pharmaceut.* **2006**, *3*, 717.
[35] P. Major, A. Lortholary, J. Hon, E. Abdi, G. Mills, H. D. Menssen, F. Yunus, R. Bell, J. Body, E. Quebe-Fehling, J. J. Seaman, *Clin. Oncol.* **2001**, *19*, 558.
[36] J. R. Berenson, *Oncologist* **2005**, *10*, 52.
[37] L. Q. Liu, Z. M. Li, X. B. Wang. *J. Beijing Norm. Univ.* **2004**, *40*, 75.
[38] H. Z. Pan, M. Sima, P. Kopecková, K. Wu, S. Q. Gao, J. H. Liu, D. Wang, S. C. Miller, J. Kopecek, *Mol. Pharmaceut.* **2008**, *5*, 548.